Version sent, 4/9/92

On Visualizing the Four-Dimensional Rigid Body

Robert McLachlan
Program in Applied Mathematics, University of Colorado at Boulder, Boulder CO 80309

It is difficult to display complicated objects in dimensions more than three and actually add to one's understanding of the object. It is not clear that the reduction to three dimensions can be done without just confusing matters. Projecting to R^3 creates artificial self-intersections; slicing loses global information. Therefore we look first at simpler objects, namely invariant sets of integrable symplectic flows or maps. The integrals tell one how to project and slice without creating self-intersections. Understanding such pictures should help when studying near-integrable cases.

The Euler-Arnol'd equations for the motion of a free rigid body in R^4 are

$$\dot{M} = [M, \Omega] \qquad M, \Omega \in so^*(4) \tag{1a}$$

$$M = J\Omega + \Omega J \qquad J = diag(J_1, J_2, J_3, J_4) \tag{1b}$$

To write explicitly in Lie-Poisson form, let $m = (M_{12}, M_{13}, M_{14}, M_{23}, M_{24}, M_{34})^T$ and ω the analagous vector for Ω. The Poisson tensor is

$$\Lambda = \begin{pmatrix} 0 & -m_4 & -m_5 & m_2 & m_3 & 0 \\ m_4 & 0 & -m_6 & -m_1 & 0 & m_3 \\ m_5 & m_6 & 0 & 0 & -m_1 & -m_2 \\ -m_2 & m_1 & 0 & 0 & -m_6 & m_5 \\ -m_3 & 0 & m_1 & m_6 & 0 & -m_4 \\ 0 & -m_3 & m_2 & -m_5 & m_4 & 0 \end{pmatrix}$$

with associated energy and Hamiltonian system

$$H = \frac{1}{2} m.\omega, \qquad \dot{m} = \Lambda(m)\nabla H(m) = \Lambda(m)\omega.$$

Note that $\Omega_{ij} = M_{ij}/(J_i + J_j)$. Generally rank$(\Lambda) = 4$ and from (1a) we see the Casimirs are tr(M^2) and tr(M^4). These may be simplified to

$$C_1 = \sum_{i=1}^{6} m_i^2 \tag{2a}$$

$$\text{and} \qquad C_2 = m_1 m_6 - m_2 m_5 + m_3 m_4 \tag{2b}$$

The dynamics takes place on four-dimensional symplectic leaves in R^6 defined by the common level sets of (2a) and (2b). Add and subtract these equations and they decouple:

$$(m_1 \pm m_6)^2 + (m_2 \mp m_5)^2 + (m_3 \pm m_4)^2 = C_1 \pm 2C_2 \tag{3}$$

showing that the symplectic leafs are isomorphic to $S^2 \times S^2$. An exception is when $C_1 = \pm 2C_2$. In this case rank $(\Lambda) = 2$ and motion is restricted to two-dimensional symplectic bones, here just one of the spheres (3). The dynamics reduces to the 3D rigid body in this case. Finally, if $C_1 = 0$ then $\Lambda = 0$ and $M \equiv 0$.

The two dynamical integrals of motion are

$$I_1 = H = \sum_{j>i} M_{ij}^2/(J_i + J_j)$$
$$I_2 = -\frac{1}{3}\left(\mathrm{tr}(J^2MM) + \mathrm{tr}(MJ^2M) + \mathrm{tr}(MMJ^2)\right) = \sum_{j>i} M_{ij}^2(J_i^2 + J_j^2)$$

There is a remarkable discrete version of this system, due to Veselov [1] (see also Moser and Veselov [2]):

$$M_{k+1} = \omega_k M_k \omega_k^T, \qquad M \in so^*(4) \tag{4a}$$
$$M_k = \omega_k^T J - J\omega_k, \qquad \omega \in SO(4) \tag{4b}$$

This defines a Poisson map $M_{k+1} = \phi(M_k)$ with all integrals C_i and I_i of the original system. Furthermore the flows coincide as $M \to 0$, and $M_{k+1} = h^{-1}\phi(hM_k)$ where h is a time-step gives a second-order symmetric integrator of (1); thus one may construct completely integrable maps approximating (1) to any order by composing several such maps with suitable time-steps (see Suzuki [3]). Equation (4b) may be solved by parameterizing $SO(4)$ near the identity by six Euler angles and solving for their sines by iteration.

Table. Fixed points of the degenerate rigid body

	Fixed point $\mathbf{m}$	C_1	C_2
(i)	$(0,0,0,\alpha,\beta,0)$	$\alpha^2+\beta^2$	0
(ii)	$(0,\alpha,\beta,0,0,0)$	$\alpha^2+\beta^2$	0
(ii)	$(\alpha,0,0,0,0,\beta)$	$\alpha^2+\beta^2$	$\alpha\beta$
(iv)	$(0,\alpha,0,0,\beta,0)$	$\alpha^2+\beta^2$	$-\alpha\beta$
(v)	$(\alpha,\beta,\gamma,k_1\gamma,-k_1\beta,k_2\alpha)$	$(1+k_1^2)(\beta^2+\gamma^2)+(1+k_2^2)\alpha^2$	$k_1(\beta^2+\gamma^2)+k_2\alpha^2$
(vi)	$(0,\alpha\beta,\beta^2,\gamma\beta,-\alpha\beta,0)$	$(\alpha^2+\beta^2)(\beta^2+\gamma^2)$	$\gamma\beta(\beta^2+\alpha^2)$

This is for $J_3 = J_4$. There is a choice of sign for k_1 and k_2, which are complicated functions of the J_i's. Solution (v) gives a circle of fixed points on leaves with $|C_2/C_1|$ between $k_1/(1+k_1^2)$ and $k_2/(1+k_2^2)$. The other circle of fixed points, (vi), exists for all C_2 but coalesces with (i), (ii) and (iv) for $C_2 = 0$ or $\pm\frac{1}{2}C_1$.

For general J_i, on a general leaf, there are 12 fixed points which are elliptic or elliptic-hyperbolic depending on the J_i's; there is also a one-parameter family of fixed points which may be elliptic or hyperbolic. To help reduce the number of dimensions, we consider the degenerate case $J_3 = J_4$, so that $\dot{m}_6 = 0$, and we have an extra integral $I_3 = m_6$. All orbits are still not periodic, however, because I_1 and I_2 are no longer functionally independent on a leaf. In the whole phase space there are four two-parameter and two three-parameter families of fixed points (see the Table). We further restrict to $C_1 = 1$, $C_2 = 0$, so that they coalesce to give twelve fixed points $\pm\mathbf{e}_i$. From Table 1 we see that $\mathbf{e}_{2,3,4,5}$ have four zero eigenvalues and the rest have only two, corresponding to the C_1 and C_2 directions. For the visualizations, we have taken $J_1 = 1$, $J_2 = 0.6$, and $J_3 = J_4 = 0.3$; this make $\mathbf{e}_1$ and $\mathbf{e}_6$ elliptic, $\mathbf{e}_2$ and $\mathbf{e}_3$ hyperbolic-zero, $\mathbf{e}_4$ and $\mathbf{e}_5$ elliptic-zero. Figure 1 shows some orbits on the symplectic leaf $S^2 \times S^2$, with $m_6 = 0.1$ and the initial condition moving farther away from the fixed point $\mathbf{e}_1$. Note $H(\mathbf{e}_1) = \frac{5}{16} \leq H \leq \frac{5}{9} = H(\mathbf{e}_6)$ for these J's.

It is hard to reduce to R^3 without creating intersections—e.g., one cannot just put angles on $S^2 \times S^2$ and drop one of them. We stick to the original coordinates (m_2, m_3, m_4) and can restrict intersections to the $m_2 = 0$ plane. Our construction is as follows. First slice by C_1, C_2 and I_3, giving a three-dimensional set Σ. Project to R^3 by $(m_1, m_2, m_3, m_4, m_5, m_6) \mapsto (m_2, m_3, m_4)$. Given (m_2, m_3, m_4), eqs. (2) give two solutions for m_1; then m_5 may be recovered from (2b). Thus the I_3-slice of the symplectic leaf may be visualized as two solid objects pinned together at their surface (where (2a) has only one solution for m_1) which we call Σ':

$$\Sigma' : \qquad m_3^2 = \frac{\left(1 - (m_2^2 + m_4^2 + m_6^2)\right)(m_2^2 + m_6^2)}{m_2^2 + m_4^2 + m_6^2}$$

This surface is shown in Figure 2a. The dynamics takes place in the interior of two such objects, and moves from one sphere to the other through its surface. By drawing only the part of any object which corresponds to one root of (2a) for m_1, we avoid self-intersections except when $m_2 = 0$, in which case one can no longer recover m_5.

Case 1. $I_3 = m_6 = 0$. In this case one case solve the C_1-C_2-I_3-H equations to get the constant-energy tori explicitly—they are graphs over an ellipse in the $m_3 = 0$ plane, which makes them easy to draw (see Figure 2b). Their $m_1 > 0$ parts foliate the interior of Σ'. For $H < H(\mathbf{e}_2)$, they stay in the illustrated half of Σ; for $H > H(\mathbf{e}_2)$, they cross over. The largest surface shown has $H = H(\mathbf{e}_2)$ and connects the fixed points $\pm e_2$ and $\pm e_3$.

This I_3-slice is further degenerate in that we have two more (not functionally independent) integrals, $I_4 = m_3/m_2$ and $I_5 = m_5/m_4$. Thus all orbits are periodic and can be shown to follow 3D rigid body dynamics. For example, Figure 3 shows the slice $m_3 = 0$, which is just the projection of the 3D rigid body's phase portrait, and Figure 4 shows different orbits on one of the constant-energy tori.

Case 2. $I_3 = m_6 \neq 0$. Now the orbits are only quasi-periodic, as shown in Figure 1. Unfortunately our graphics run into problems here—the C_1-C_2-I_3-H equations are unwieldy to solve in such a way that one can draw the solutions. Two possible approaches would be to diagonalize the equations into the form $x^2 + y^2 = 1$, $w^2 + z^2 = 1$ giving nice coordinates on the tori (which is also impractical), or to draw the surfaces numerically as constant-H isosurfaces, which only requires solving the first three equations, but this software is not available to me.

Figure 5 shows Σ' in the case $m_6 = 0.1$ and one orbit, fairly close to the elliptic fixed point $\mathbf{e}_1$. Note its two false intersections where it crosses $m_2 = 0$.

References

[1] Veselov, A.P., "Integrable Discrete-Time Systems and Difference Operators," *Funct. Anal. App.* **22** (1988), 83–93.

[2] Moser, J. and Veselov, A.P., "Discrete Versions of some Classical Integrable Systems and Factorization of Matrix Polynomials," *Comm. Math. Phys.* **139**(2), p. 217.

[3] Suzuki, M., "General theory of fractal path integrals with applications to many-body theories and statistical physics," *J. Math. Phys.* **32**(2) (1991), 400–407.

Figure captions

Figure 1. Orbits on a symplectic leaf $\cong S^2 \times S^2$. Here $m_6 \equiv 0.1$, and the initial condition is $m_2 = m_5 = 0$, m_1, m_3, and m_4 recovered from the integrals $C_1 = 1$, $C_2 = 0$, and H.

Figure 2. (top) Surface Σ' when $m_6 = 0$; (bottom) foliation of the interior of Σ' by constant-energy surfaces. Three of the fixed points $\mathbf{e}_2$, $\mathbf{e}_3$, and $\mathbf{e}_4$, are marked; $\mathbf{e}_1$ is at the origin in this projection.

Figure 3. Energy surfaces in the $m_3 = 0$ plane—these are just the orbits of a 3D rigid body in orthogonal projection. Notice how this figure fits into the cutaway section of Figure 2b.

Figure 4. Orbits on the surface $m_6 = 0$, $H = 0.34$.

Figure 5. (top) Surface Σ' when $m_6 = 0.1$ (it is no longer pinched, but the projection to (m_2, m_3, m_4) is still singular on $m_2 = 0$); (bottom) an orbit as in Figure 1 but with $m_6 = 0.1$—a piece of Σ' is also shown.

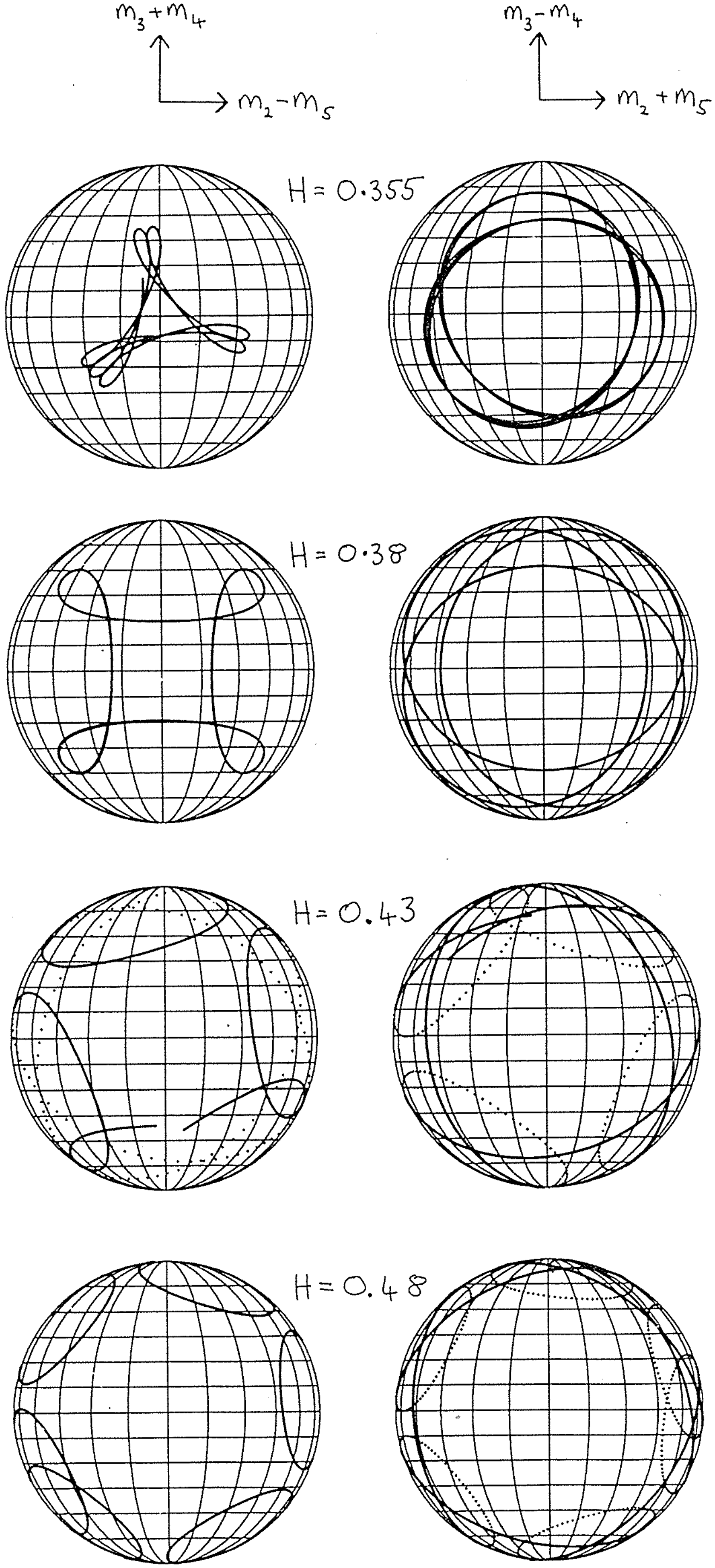
$m_3 + m_4$
$m_2 - m_5$
$m_3 - m_4$
$m_2 + m_5$
H = 0.355
H = 0.38
H = 0.43
H = 0.48

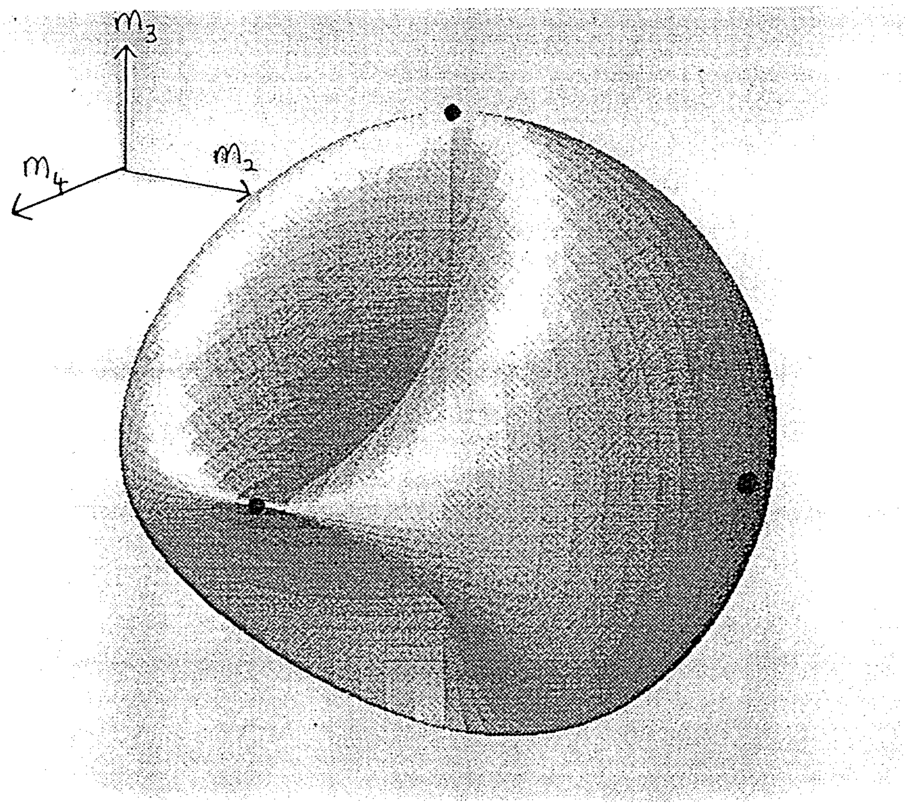
m_3
m_4
m_2

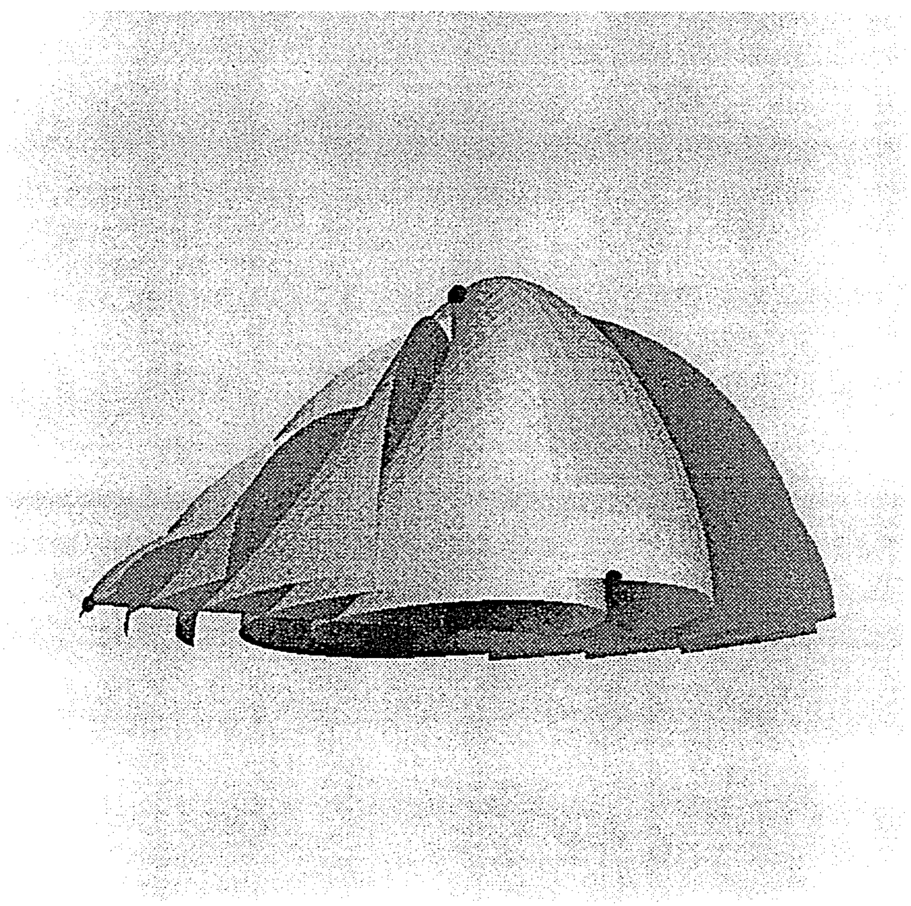

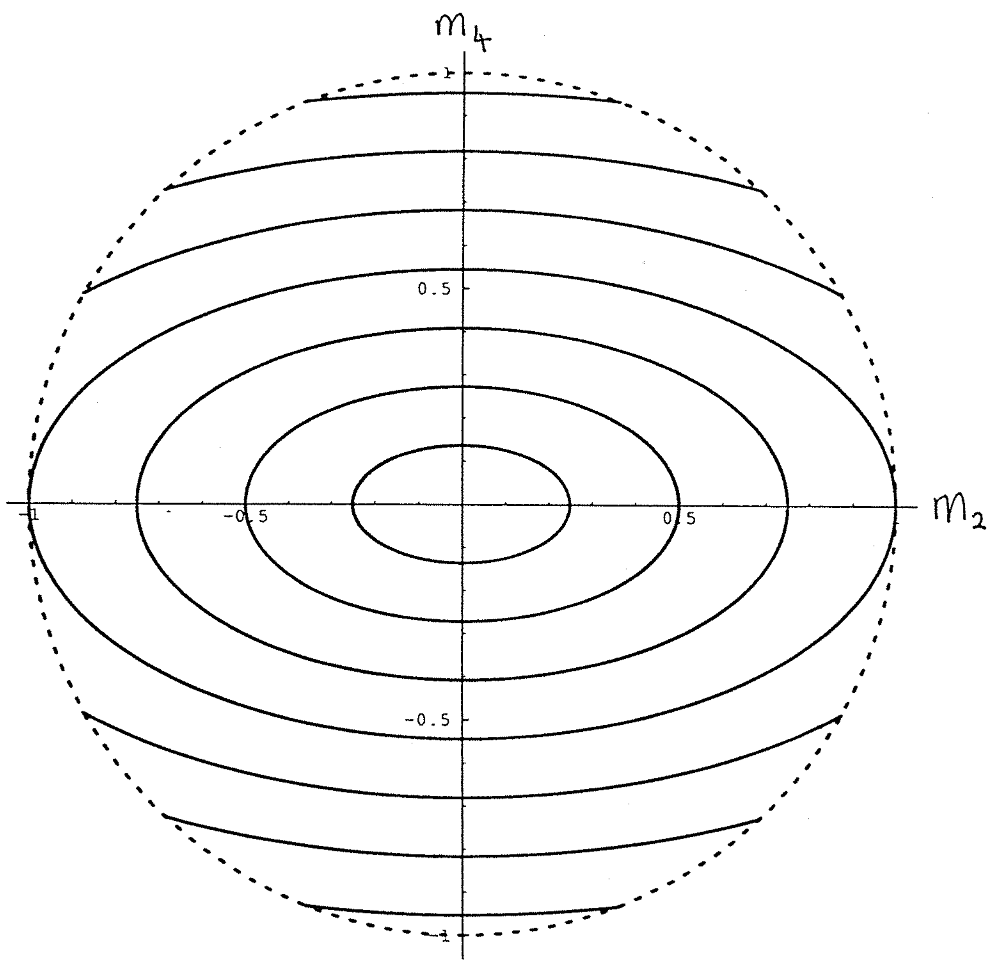
m_4
1
0.5
-0.5
-1
-1
-0.5
0.5
m_2